World Scientific
www.worldscientific.com

ON THE POWER EFFICIENCY OF CASCODE COMPENSATION OVER MILLER COMPENSATION IN TWO-STAGE OPERATIONAL AMPLIFIERS

HAMED AMINZADEH* and REZA LOTFI

*Integrated Systems Laboratory, EE Department,
Ferdowsi University of Mashhad, Azadi Square,
Mashhad, Khorasan, I. R. Iran
haminzadeh@ieee.org

Optimization of power consumption is one of the main design challenges in today's low-power high-speed analog integrated circuits. In this paper, two popular techniques to stabilize two-stage operational amplifiers, namely, Miller and cascode compensations are compared from power efficiency point of view. To accomplish this, cascode-compensated topologies are basically analyzed to derive the required equations for the comparison. In the analysis, a new method to take into account the effect of transfer function zeros is proposed. By assuming that the zeros' magnitudes are fairly nondominant, the method increases the accuracy of the analyses. The relationships show that for the same specifications, cascode compensation is more power-efficient than Miller compensation, especially for heavy capacitive loads. This has been confirmed by SPICE simulations.

Keywords: Frequency compensation; low-power design; operational amplifiers; stability.

1. Introduction

Power consumption is one of the main challenging issues in modern electronic equipments. Its reduction looks like to be more challenging when designing low-voltage analog integrated circuits in deep sub-micron technologies, especially operational amplifiers (opamps). At the first glance, reduction of supply voltages and transistor dimensions seems to be effective in lowering opamp power consumption. However, as there will be less room for the signal, to keep the same signal-to-noise ratio the power should be increased. Moreover, as lower available power supplies prevent the designers to stack adequate transistors upon each other, it becomes quite difficult to satisfy both the required DC gain and voltage swing with single-stage amplifiers. As a result, multistage opamps with more power-hungry branches might be inevitable.[1]

Two-stage opamps are used widely in industry to achieve high DC gain and high output voltage swing together. To avoid instability in the negative feedback loop, the opamp frequency response should be appropriately compensated. Several

compensation techniques have been proposed to stabilize a two-stage amplifier.[2,3] For a particular value of power consumption, each technique makes a trade-off between stability and bandwidth. How much the trade-off is determines the benefit of one scheme over another. To compare the two popular compensation techniques for two-stage opamps, namely, Miller and cascode compensations from this point of view, a new analysis has been performed in this paper.

When Miller compensation is applied to a two-stage opamp, a compensation capacitor is placed between the input and output of second stage. The capacitor has a pole-splitting action which moves one pole to lower frequencies and the other one to higher frequencies. This increases the closed-loop stability, but lowers the opamp bandwidth. In general, the main drawbacks of Miller compensation are low power efficiency, low power supply rejection ratio (PSRR), and large value of required compensation capacitor. The feedforward current flow through the compensation capacitor toward the output is another issue in Miller-compensated amplifiers.[4] The current introduces a right-half-plane (RHP) zero to the transfer function which reduces the closed-loop stability. The reason why this feedforward current degrades the stability is that it tries to pass the signal to the opamp output by bypassing the second stage. This nullifies the 180° phase shift by the second stage and reverses the output polarity. Equivalently, it forces the negative feedback to become positive. Hence, the output sign inversion occurs at lower frequencies with higher absolute loop-gain value and lower phase margin. A nulling resistor is applied in series with the compensation capacitor to avoid bypassing the second stage with this current.[5] The resistor increases the feedforward path impedance and equivalently moves the RHP zero to higher frequencies. However, in practice, the value of the resistor is affected by temperature and other variations in device fabrication, which results in more variations in opamp's stability. Due to this, another method to reduce the effect of the RHP zero, called as cascode compensation is proposed. Instead of a nulling resistor, it employs a current buffer in series with the compensation capacitor. The current buffer tries to decrease the feedforward current by conducting it directly to the second-stage input. Correspondingly, it tries to push the RHP zero to higher frequencies.[4] Compared to the previous method, it offers some advantages. First, as the parameters of current buffers are less sensitive to the variations, the structure robustness increases. Second, for a particular bandwidth, it results in higher PSRR and lower power consumption. Nevertheless, these advantages are at the cost of higher complexity during the design and optimization of these topologies. Perhaps, the main reason for such complexity is the increase in the order of the system due to the practical implementation of current buffers. Correspondingly, the analysis of such systems becomes more complicated.

The aim of the analysis performed in this paper is to compare Miller compensation with cascode compensation from the power efficiency point of view. To do this, the ambiguous relationships between bandwidth and stability of a two-stage cascode-compensated opamp are obtained. It has been hard to observe the effect of zeros in the analysis of such structures, and thus most previous closed-loop based studies neglect their effect.[3,4,6–8] Assuming that zeros are located at high

frequencies, the analysis in this work does not ignore them. This is done based on the zeros Taylor expansion, which will be explained later.

The analysis in this paper is based on the meaningful and user-friendly open-loop parameters instead of their closed-loop equivalents.[6,7] Open-loop parameters are formerly proved to be useful in analyzing three-stage amplifiers.[9,10]

The rest of the paper is organized as follows: In Sec. 2, the details of the analysis for two-stage cascode-compensated opamps are presented. The same well-known analysis for two-stage Miller-compensated opamps is brought in Sec. 3. Section 4 compares the two structures from power point of view. Simulation results in $0.25 \, \mu$m CMOS technology are presented in Sec. 5, and finally the conclusion is given in Sec. 6.

2. Two-Stage Cascode-Compensated Opamps

Figure 1 shows a two-stage opamp composed of a folded-cascode amplifier as the first stage and a common-source amplifier as its second stage. It employs cascode compensation scheme to avoid closed-loop instability. This topology has been chosen typically and the analyses could be applied to any other two-stage fully-differential or single-ended opamps. Figure 2 shows the small-signal equivalent, where C_A, C_B, and C_L and R_{oA}, R_{oB}, and R_L are the total capacitances and resistances seen at nodes A, B and V_O, respectively. After resolving the small-signal set of equations, making reasonable simplifications, and performing some routine algebra, the small-signal transfer function is obtained as follows[4]:

$$A_V(s) \cong \frac{g_{mi}g_{mL}R_{oB}R_L(1 - s^2/(g_{mB}g_{mL}/C_BC_C))}{(1 + g_{mL}R_LR_{oB}C_Cs)(1 + (C_B(C_L + C_C)/g_{mL}C_C)s + (C_LC_B/g_{mB}g_{mL})s^2)}. \tag{1}$$

The transfer function has one real dominant pole and two nondominant poles. Nondominant poles are complex when their damping factor is less than unity
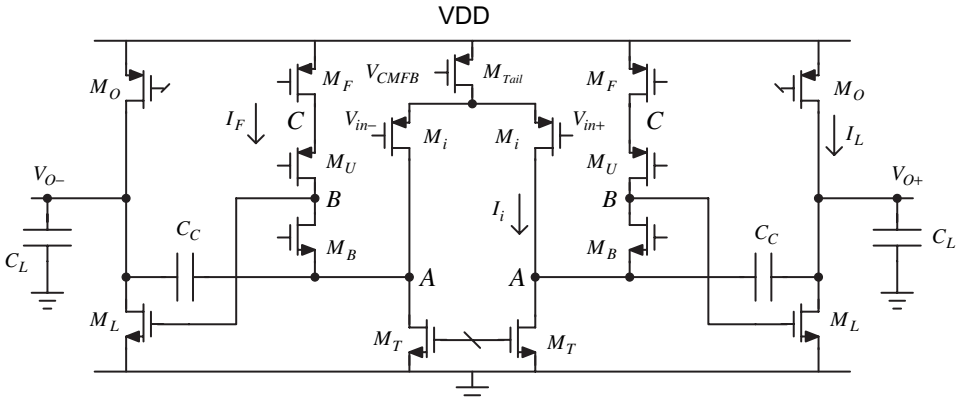

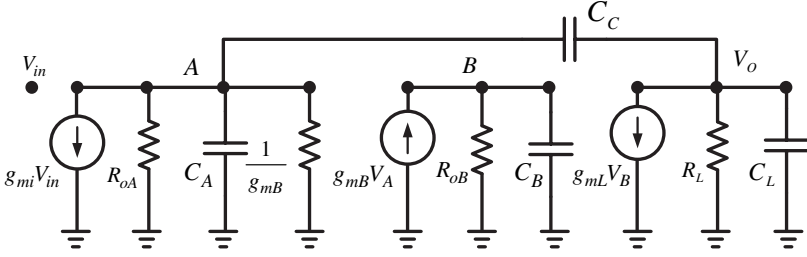Fig. 1. A two-stage fully-differential opamp with cascode compensation.

Fig. 2.   Small-signal differential mode half-circuit.

($\xi < 1$). The transfer function also has two zeros: one is located at RHP and the other one is located at the left-half-plane (LHP).

Previously performed analyses in literature[3,4,6–8] were based upon the assumption that the effect of zeros is negligible in the output response. As it is seen in Eq. (1), the magnitude of zeros can be even comparable with the magnitude of nondominant poles. Thus, their effect should also be considered appropriately. Equation (1) can be rewritten in the following symbolic form:

$$A_V(s) = \frac{A_{\mathrm{DC}}(1 - s^2/z^2)}{(1 + s/\omega_0)(1 + s(2\xi/\omega_n) + s^2/\omega_n^2)}$$

$$\cong \frac{1 - s^2/z^2}{(s/GBW_{\mathrm{Cascode}})(1 + s(2\xi/\omega_n) + s^2/\omega_n^2)}, \tag{2}$$

where A_{DC}, $z_{1,2} = \pm|z|$ and ω_0 are the opamp open-loop DC gain, the magnitude of zeros, and the magnitude of dominant pole, respectively. GBW_{Cascode} represents the opamp gain-bandwidth frequency, where $|A_V(j\omega)|$ becomes equal to unity. These parameters are related to small-signal parameters according to the following equations:

$$A_{\mathrm{DC}} = g_{mi}g_{mL}R_{oB}R_L, \tag{3}$$

$$z_{1,2} = \pm\sqrt{\frac{C_B C_C}{g_{mB}g_{mL}}}, \tag{4}$$

$$\omega_0 = \frac{1}{g_{mL}R_L R_{oB}C_C}, \tag{5}$$

$$GBW_{\mathrm{Cascode}} = A_{\mathrm{DC}}\omega_0 = \frac{g_{mi}}{C_C}. \tag{6}$$

The two parameters ξ and ω_n are the nondominant poles damping factor and natural frequency, respectively. Comparing Eq. (1) with Eq. (2), it can be found that

$$\xi = \frac{1}{2}\sqrt{\frac{g_{mB}C_B}{g_{mL}C_L}} \cdot \left(1 + \frac{C_L}{C_C}\right), \quad \omega_n = \sqrt{\frac{g_{mB}g_{mL}}{C_L C_B}}. \tag{7}$$

It is relatively hard to observe the effect of zeros in the transfer function as shown in Eq. (2). An elegant and efficient way to make the analysis more accurate is to properly model the effect of zeros in the generic second-order polynomial of the denominator. Hence, the new values of damping factor (ξ) and natural frequency (ω_n) called as effective damping factor (ξ') and effective natural frequency (ω'_n) can be defined such that the effects of zeros are taken into account:

$$\frac{1 - s^2/z^2}{1 + s(2\xi/\omega_n) + s^2/\omega_n^2} = \frac{1}{1 + s(2\xi'/\omega'_n) + s^2/\omega'^2_n} . \tag{8}$$

The equation in the form of Eq. (8) does not yield straightforward relations between effective damping factor and effective natural frequency with small-signal parameters. However, Taylor expansion of zeros can be used to rewrite Eq. (8) as:

$$1 + s\left(\frac{2\xi'}{\omega'_n}\right) + \frac{s^2}{\omega'^2_n} = \frac{1 + s(2\xi/\omega_n) + s^2/\omega_n^2}{1 - s^2/z^2}$$
$$= \left(1 + s\left(\frac{2\xi}{\omega_n}\right) + \frac{s^2}{\omega_n^2}\right) \cdot \left(1 + \frac{s^2}{z^2} + \cdots\right) . \tag{9}$$

By ignoring higher than second-order terms that are very small when the zeros are located at high frequencies, Eq. (9) is simplified into

$$1 + s\left(\frac{2\xi'}{\omega'_n}\right) + \frac{s^2}{\omega'^2_n}$$
$$\approx 1 + s\left(\frac{2\xi}{\omega_n}\right) + s^2\left(\frac{1}{\omega_n^2} + \frac{1}{z^2}\right) . \tag{10}$$

Approximation (10) may not hold true in case the zeros are located at low frequencies, in which higher order terms are important. However, this approximation is the key point to increase the accuracy of the derived equations. Equating the corresponding coefficients in Eq. (10), the relationship between the new effective damping factor and natural frequency with their old counterparts is obtained:

$$\frac{1}{\omega'^2_n} = \frac{1}{\omega_n^2} + \frac{1}{z^2},$$
$$\frac{2\xi'}{\omega'_n} = \frac{2\xi}{\omega_n}. \tag{11}$$

Figure 3 depicts the concept of how the effect of zeros can be embedded into the damping factor and natural frequency. It shows that the effect of zeros, together with nondominant pole magnitudes can be combined to define the effective poles with new magnitudes. The new pole locations can be found by defining an effective damping factor and an effective natural frequency for them.
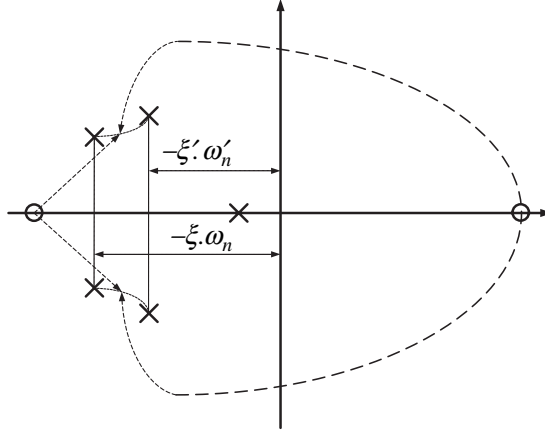
Fig. 3.   Modeling the approximate effect of zeros on the location of nondominant poles. (Two new parameters called as effective damping factor and effective natural frequency are defined.)

Substituting Eq. (7) into Eq. (11) and rearranging, it can be shown that

$$\xi' = \frac{1}{2}\sqrt{\frac{g_{mB}C_B(C_C + C_L)}{g_{mL}C_C^2}}, \quad \omega_n' = \sqrt{\frac{g_{mB}g_{mL}}{C_B(C_C + C_L)}}. \tag{12}$$

Equation (12) shows that ξ' and ω_n' can directly be controlled by changing the values of C_C, g_{mB}, and g_{mL}. There is however less control on the value of C_B, the parasitic capacitance of the first stage output, because it is a function of the transistors' parasitic capacitances which are related to their dimensions and biasing points.

ξ' and ω_n' have a major effect on the settling response of the amplifier. These two parameters should be carefully determined. Their product result (which will be used later) is as follows:

$$\xi'\omega_n' = \frac{1}{2}\frac{g_{mB}}{C_C}. \tag{13}$$

In simulations, the relationship between ξ and ξ' is helpful to indirectly determine ξ' from ξ. Comparing Eq. (7) with Eq. (12) it can be shown that

$$\frac{\xi'}{\xi} = \sqrt{\frac{C_L}{C_C + C_L}}. \tag{14}$$

Equation (14) proves the inaccuracy of foregoing methodologies. It shows that the difference between ξ (which was conventionally used when ignoring the effect of zeros) and ξ' (which takes into account the effect of zeros) could be remarkable. It also shows that the conventional approach in the literature to ignore the effect of zeros may result in an unacceptable deviation between analytical and measurement results.

According to the proposed model, the transfer function will be as follows:

$$A_V(s) \cong \frac{A_{\mathrm{DC}}}{(1 + s/\omega_0)(1 + s(2\xi'/\omega'_n) + s^2/\omega'^2_n)} \, . \tag{15}$$

The phase margin is defined as the relative distance between the phase of the amplifier at the loop-gain transient frequency (where $|\beta \cdot A_V(j\omega)|$ becomes equal to unity) and -180. If the loop-gain transient frequency is approximated as $\beta \cdot GBW_{\mathrm{Cascode}}$ (similar to a first-order system), this parameter can be approximated as follows:

$$\phi_M = 180 - \tan^{-1}\left(\frac{\beta \cdot GBW_{\mathrm{Cascode}}}{\omega_0}\right) - \tan^{-1}\left(\frac{2\xi'(\beta \cdot GBW_{\mathrm{Cascode}}/\omega'_n)}{1 - (\beta \cdot GBW_{\mathrm{Cascode}}/\omega'_n)^2}\right), \tag{16}$$

where β is the feedback factor of the closed-loop amplifier. Since, after compensation, the first dominant pole is located at very low frequencies, the relative distance between its location and the loop-gain transient frequency becomes relatively large. Hence, the ratio $\beta \cdot GBW_{\mathrm{Cascode}}/\omega_0$ tends to infinity and we can write

$$\phi_M = 90 - \tan^{-1}\left(\frac{2\xi'_0(\beta \cdot GBW_{\mathrm{Cascode}}/\omega'_{n0})}{1 - (\beta \cdot GBW_{\mathrm{Cascode}}/\omega'_{n0})^2}\right) . \tag{17}$$

According to Eq. (17), it can be shown that

$$\tan(\phi_M) = \left(\frac{1 - (\beta \cdot GBW_{\mathrm{Cascode}}/\omega'_{n0})^2}{2\xi'_0(\beta \cdot GBW_{\mathrm{Cascode}}/\omega'_{n0})}\right) . \tag{18}$$

Substituting ω'_n and $\xi'\omega'_n$ from Eqs. (12) and (13) into Eq. (18), the two following expressions for the GBW_{Cascode} are obtained:

$$GBW_{\mathrm{Cascode}} = \frac{1}{\beta}\sqrt{\frac{g_{mB}g_{mL}}{C_B(C_C + C_L)}} \frac{1}{\xi'\tan(\phi_M) + \sqrt{1 + \xi'^2\tan^2(\phi_M)}}, \tag{19}$$

$$GBW_{\mathrm{Cascode}} = \frac{1}{\beta}\frac{g_{mB}}{2\xi'C_C(\xi'\tan(\phi_M) + \sqrt{1 + \xi'^2\tan^2(\phi_M)})} . \tag{20}$$

Given g_{mB}, C_C, and β, the two equations (19) and (20) predict that the lower effective damping factor would result in a higher GBW_{Cascode}. However, for the same value of phase margin, the relative distance between this parameter and ω'_n decreases. This could finally cause an induced peak in the interested frequency region (from low frequencies up to $\beta \cdot GBW_{\mathrm{Cascode}}$) and significantly degrade the closed-loop stability and gain margin (GM). Perhaps, keeping $\xi' \tan(\varphi_M)$ greater than a threshold around unity is essential for the closed-loop stability and a lower ξ' should be compensated by a higher phase margin.

3. Two-Stage Miller-Compensated Opamps

Figure 4 shows a two-stage Miller-compensated operational amplifier and its small-signal equivalent. Similar notations as in the previous section are used to denote the parameters. As it is highlighted in the introduction, a nulling resistor (R_C) is applied in series with the compensation capacitor to nullify the effect of RHP zero and to push it to infinity. After compensation, assuming that the RHP zero is moved to high frequencies, the transfer function will be[1,2,5]:

$$A_V(s) = \frac{g_{mi}g_{mL}R_{oB}R_L}{(1+g_{mL}R_LR_{oB}C_Cs)(1+(C_L/g_{mL})s)} = \frac{A_{\mathrm{DC}}}{(1+s/\omega_0)(1+s/\omega_1)}$$

$$\cong \frac{1}{(s/GBW_{\mathrm{Miller}})(1+s/\omega_1)}, \tag{21}$$

where GBW_{Miller} has the same definition as that of GBW_{Cascode}. According to Eq. (21), the relationship between GBW_{Miller} and phase margin becomes:

$$\varphi_M \cong 90 - \tan^{-1}\left(\frac{\beta \cdot GBW_{\mathrm{Miller}}}{g_{mL}/C_L}\right). \tag{22}$$
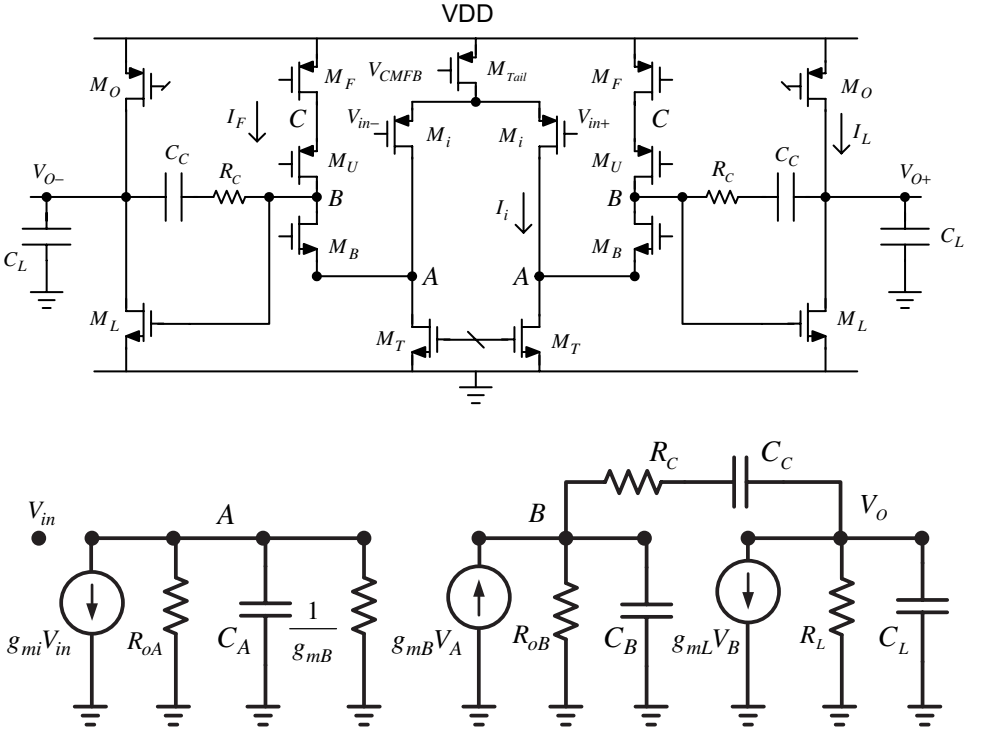

Fig. 4.   A two-stage Miller-compensated opamp and its small-signal equivalent.

Combining Eqs. (21) and (22), we can obtain

$$GBW_{\text{Miller}} = \frac{g_{mi}}{C_C} \cong \frac{1}{\beta} \frac{g_{mL}}{C_L \tan(\varphi_M)} . \tag{23}$$

4. Comparison Between Power Consumptions

The performed analysis in Secs. 2 and 3 makes it possible to compare cascode compensation and Miller compensation with nulling resistor based on their consuming power.

As it is clear, for a constant overdrive voltage, the transconductance of MOS transistors is linearly proportional to their bias currents (when biased in strong inversion region).

It can be shown that for the same stability margins, the total power of an amplifier is linearly proportional to its gain-bandwidth (GBW). In Fig. 3, assuming that the current of folded branch (I_{F}) is proportional to the input current (i.e., $I_{\text{F}} = \alpha I_{\text{i}}$), the power consumption value (P) would be

$$P = 2 \cdot VDD \cdot (I_{\text{i}} + \alpha I_{\text{i}} + I_L) = VDD \cdot ((1 + \alpha)g_{mi} \cdot V_{\text{ovi}} + g_{mL} \cdot V_{\text{ovL}}), \tag{24}$$

where the notation V_{ov} is used to denote the overdrive voltage of each transistor. Substituting Eq. (23) into Eq. (24), we can obtain

$$P = VDD \cdot ((1 + \alpha)C_C \cdot V_{\text{ovi}} + \beta \cdot C_L \cdot \tan(\varphi_M) \cdot V_{\text{ovL}}) \cdot GBW_{\text{Miller}} . \tag{25}$$

As can be seen, for a particular load capacitor, feedback factor and stability margins (unchanged values of C_C and φ_M) power consumption is linearly proportional to the gain-bandwidth (GBW_{Miller}). The same consequence can be achieved for cascode compensation using Eqs. (6), (19), and (20), and for constant ξ', C_C, and φ_M.

Based on these facts, comparison between power consumption of the two topologies is equivalent to comparing them from the GBW viewpoint. The approach in three-stage opamps is to compare the GBWs of two topologies when their power and stability margins are identical.[10–12] The same figure of merit (FOM) (the ratio between GBWs for the same amount of stability margins and power) will be applied here.

By defining m as the ratio of compensation capacitor to the load capacitor in cascode compensation (which is between 0 and 1 in typical designs) and using Eqs. (19) and (23), the highlighted ratio (R) is expressed as:

$$m = \frac{C_{C(\text{Cascode})}}{C_L}, \tag{26}$$

$$\frac{GBW_{\text{Cascode}}}{GBW_{\text{Miller}}} = R, \tag{27}$$

$$R = \frac{1}{\sqrt{1+m}} \frac{\tan(\varphi_M)}{\xi' \tan(\varphi_M) + \sqrt{1 + \xi'^2 \tan^2(\varphi_M)}} \sqrt{\frac{g_{mB}}{g_{mL}}} \sqrt{\frac{C_L}{C_B}}. \tag{28}$$

In case, R being greater than unity, cascode compensation achieves higher bandwidth than Miller compensation for the same amount of power. However, R can be made larger, which is the case when the amplifier is loaded by a large capacitance, as the ratio is proportional to $\sqrt{C_L}$. For unchanged stability margins (ξ' and φ_M), maximizing g_{mB}, the transconductance of M_B, with respect to g_{mL}, the transconductance of M_L and minimizing the second-stage input node parasitic capacitance (C_B) make this approach more efficient.

As it is seen in Eq. (25), in optimized designs, achieving higher GBWs for fixed stability margins is only possible by increasing the power. Consequently, Eq. (28) predicts that for a particular gain-bandwidth, cascode compensation is more power-efficient than Miller compensation, especially for heavy capacitive loads.

5. Simulation Results

To verify the accuracy of the derived equations and to compare the two structures, several simulations were performed by $0.25\,\mu$m BSIM3v3 level 49 mixed-signal CMOS HSPICE models. For a unity-gain buffer, a small on-chip opamp was required to drive a $8.5\,$pF capacitive load. For the available amount of power, the opamp gain-bandwidth product which has effects on the distortion of the delivered signal to the load was important. Two opamps with the structures shown in Figs. 1 and 4 were designed and precisely simulated for this application. To compare the effectiveness of the two compensation techniques, the opamp core in both the designs was kept unchanged, and only the compensation scheme was changed. Table 1 shows the small-signal parameters and device sizes of the designed opamp.

The first opamp was compensated by the cascode compensation scheme. The stability margins (ξ' and φ_M) were determined at first. As it has been demonstrated in third-order systems, to achieve the maximum closed-loop unity-feedback flat band the damping factor (or effective damping factor according to our analysis) and the phase margin should be adopted equal to 0.7 and 60°, respectively.[6,7] The compensation capacitor and devices transconductances were appropriately changed according to Eqs. (6), (19), and (20) to set these two parameters. With $\xi' = 0.7$

Table 1.   Device sizes and circuit parameters.

Device	(W/L)	Transconductance (g_m) mA/V	Parameter	Value
M_{i}	90/0.25	3.81	R_{oA}	$0.3\,$kΩ
M_T	80/0.4	10.59	R_{oB}	$8\,$kΩ
M_L	100/0.25	12.6	R_L	$1\,$kΩ
M_B	180/0.25	14.9	C_A	$0.81\,$pF
M_U	200/0.25	8.48	C_B	$0.79\,$pF
M_F	250/0.5	8.07	C_L	$8.5\,$pF
M_O	200/0.5	7.53		
M_{Tail}	100/0.25	5.19		

Table 2.   Simulated and calculated results.

Parameter	Expected value	Cascode-compensated topology	Expected value	Miller-compensated topology
Supply voltage (VDD)		1.5 V		
Gain-bandwidth product (GBW)	300 MHz	300 MHz	183 MHz	167 MHz
Phase margin (PM)	60°	60°	60°	60°
Effective damping factor (ξ')	0.707	0.612	—	—
Open-loop DC gain (A_{DC})	60 dB	62 dB	60 dB	62 dB
Power consumption		11.5 mW		

and $\varphi_M = 60°$, an approximate 300 MHz gain-bandwidth with 2 pF compensation capacitor was achieved.

The second opamp was compensated by Miller compensation scheme. To obtain an identical stability ($\varphi_M = 60°$), the compensation capacitor was connected to node B (instead of A) and was increased to 3.3 pF. A 90 Ω nulling resistor was also added in series with the compensation capacitor to push the RHP zero to infinity.

A comparison between simulation and calculation results has been made in Table 2. The results confirm an acceptable agreement between the simulations and Eq. (23). The loop-gain frequency responses for both the cases are shown in Fig. 5.

Using the simulation-extracted small-signal parameters shown in Table 1, the ratio of R defined by Eq. (28) is obtained as follows:

$$\frac{GBW_{\text{Cascode}}}{GBW_{\text{Miller}}} = \frac{0.6}{\sqrt{1+0.3}}\sqrt{\frac{14.9\,\text{mA/V}}{12.6\,\text{mA/V}}}\sqrt{\frac{8.5\,\text{pF}}{0.79\,\text{pF}}} \cong 1.88\,.$$

This prediction is confirmed by simulation, because Fig. 4 and Table 2 show that the ratio is:

$$\frac{GBW_{\text{Cascode}}}{GBW_{\text{Miller}}} = \frac{300\,\text{MHz}}{167\,\text{MHz}} = 1.79\,.$$

6. Conclusion

In this paper, two popular techniques to stabilize the two-stage operational amplifiers, namely Miller and cascode compensations are compared from power efficiency viewpoint. Cascode compensation is basically analyzed to derive the required equations. A new method to take into account the effect of transfer function zeros by the aid of their Taylor expansion is applied. The results show that cascode compensation is more power-efficient than Miller compensation, especially for heavy capacitive loads. This is a very important result to determine the type of
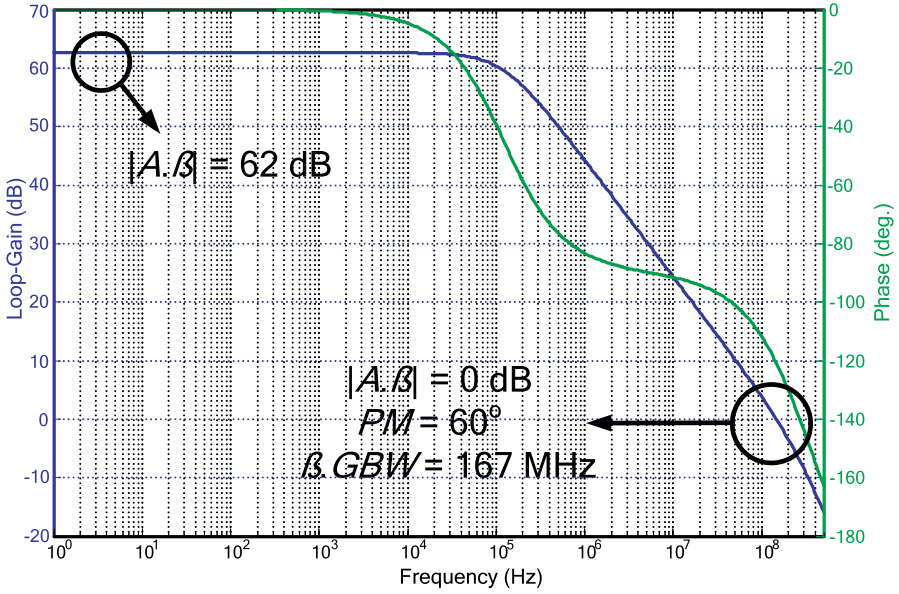
(a)
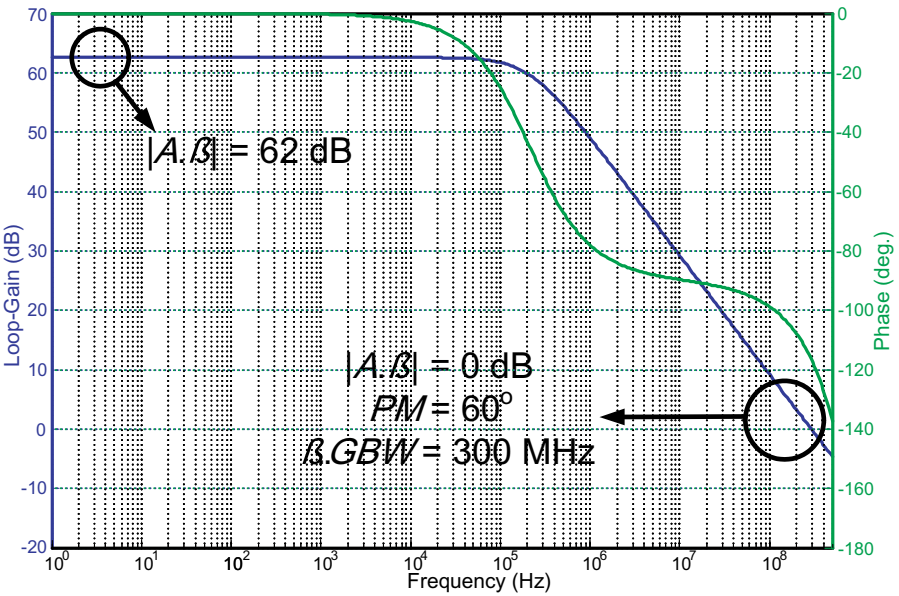
(b)

Fig. 5.   Frequency response of the opamps after compensation: (a) Miller compensation loop-gain and (b) cascode-compensation loop-gain.

compensation of the amplifier according to the load, design complexity, and power consumption.

References

1. B. Razavi, *Design of Analog CMOS Integrated Circuits* (McGraw-Hill, 2001).
2. R. G. H. Eschauzier and J. H. Huijsing, *Frequency Compensation Techniques for Low-Power Operational Amplifiers* (Kluwer Academic Publishers, 1995).
3. B. K. Ahuja, An improved frequency compensation technique for CMOS operational amplifiers, *IEEE J. Solid-State Circuits* **18** (1983) 629–633.
4. P. J. Hurst *et al.*, Miller compensation using current buffers in fully differential CMOS two-stage operational amplifiers, *IEEE Trans. Circuits Syst. I: Fund. Theor. Appl.* **51** (2004) 275–285.
5. K. N. Leung and P. K. T. Mok, Analysis of multistage amplifier frequency compensation, *IEEE Trans. Circuits Syst. I: Fund. Theor. Appl.* **48** (2001) 1041–1056.
6. A. Feldman, High-speed, low-power sigma-delta modulators for RF base-band channel applications, PhD. dissertation, University of California, Berkeley (1997).
7. R. Lotfi, M. Taherzadeh, M. Y. Azizi and O. Shoaei, Low-power design for low-voltage fast-settling operational amplifier in switched capacitor applications, *Integration, the VLSI J.* **36** (2003) 175–189.
8. M. Yavari, O. Shoaei and F. Svelto, Hybrid cascode compensation for two-stage CMOS operational amplifiers, *Proc. IEEE Int. Symp. Circuits and Systems* (2005), pp. 1565–1568.
9. G. Palumbo and S. Pennisi, Design methodology and advances in nested-Miller compensation, *IEEE Trans. Circuits Syst. I: Fund. Theor. Appl.* **49** (2002) 893–903.
10. A. Pugliese, G. Cappuccino and G. Cocorullo, Nested Miller compensation capacitor sizing rules for fast-settling amplifier design, *IEE Electron. Lett.* **41** (2005) 573–575.
11. J. Ramos and M. Steyaert, Three stage amplifier with positive feedback compensation scheme, *Proc. IEEE Custom Integrated Circuits Conf.* (1999), pp. 333–336.
12. K. N. Leung *et al.*, Damping-factor-control frequency compensation technique for low-voltage low-power large capacitive load applications, *Proc. IEEE Int. Solid-State Circuits Conf.* (1999), pp. 158–159.